The population of metastable states as a probe of relativistic-energy fragmentation reactions

A.M. Denis Bacelar,[1] A. M. Bruce,[1] Zs. Podolyák,[2] N. Al-Dahan,[2] M. Górska,[3] S. Lalkovski,[1,4] S. Pietri,[3] M.V. Ricciardi,[3] A. Algora,[5,6] N. Alkhomashi,[2] J. Benlliure,[7] P. Boutachkov,[3] A. Bracco,[8] E. Calore,[9] E. Casarejos,[10] I.J. Cullen,[2] A.Y. Deo,[2] P. Detistov,[4,11] Zs. Dombradi,[6] C. Domingo-Pardo,[3] M. Doncel,[11] F. Farinon,[3] G.F. Farrelly,[2] H. Geissel,[3] W. Gelletly,[2] J. Gerl,[3] N. Goel,[3] J. Gręboszz,[3,12] R. Hoischen,[3,13] I. Kojouharov,[3] N. Kurz,[3] S. Leoni,[8] F. Molina,[5,*] D. Montanari,[8] A.I. Morales,[7] A. Musumarra,[14] D.R. Napoli,[9] R. Nicolini,[8] C. Nociforo,[3] A. Prochazka,[3] W. Prokopowicz,[3] P.H. Regan,[2] B. Rubio,[5] D. Rudolph,[13] K.-H. Schmidt,[3] H. Schaffner,[3] S.J. Steer,[2] K. Steiger,[15] P. Strmen,[16] T.P.D. Swan,[2] I. Szarka,[16] J.J. Valiente-Dobón,[9] S. Verma,[7] P.M. Walker,[2] H. Weick,[3] and H.J. Wollersheim[3]

[1] *School of Computing, Engineering and Mathematics, University of Brighton, Brighton BN2 4GJ, UK.*
[2] *Department of Physics, University of Surrey, Guildford GU2 7XH, UK*
[3] *GSI Helmholtzzentrum für Schwerionenforschung, Planckstr 1, D-64291 Darmstadt, Germany*
[4] *Dept of Physics, University of Sofia, 1164 Sofia, Bulgaria*
[5] *Instituto de Física Corpuscular, CSIC- Univ. de Valencia, E-40071 Valencia, Spain*
[6] *Institute of Nuclear Research of the Hungarian Academy of Sciences, P.O. Box 51, Debrecen, 4001, Hungary*
[7] *Universidad de Santiago de Compostela, 15706, Spain*
[8] *Department of Physics, Università degli Studi di Milano and INFN, 20133 Milano, Italy*
[9] *INFN-Laboratori Nazionali di Legnaro, Italy*
[10] *University of Vigo, E-36310, Vigo, Spain*
[11] *Laboratorio de Radiaciones Ionizantes, Universidad de Salamanca, 37008, Spain.*
[12] *Niewodniczański Institute of Nuclear Physics, Polish Academy of Science, ul. Radzikowskiego 152, Krakow 31-342, Poland*
[13] *Department of Physics, Lund University, 22100 Lund, Sweden*
[14] *INFN-Laboratori Nazionali del Sud, via S.Sofia 62, 95125 Catania, Italy*
[15] *Physik-Department E12, Technische Universität München, D-85748 Garching, Germany*
[16] *Bratislava Faculty of Mathematics and Physics, Comenius University, 84215 Bratislava, Slovak Republic*

(Dated: March 28, 2013)

Isomeric ratios have been measured for high-spin states in $^{198,200,206,208}_{84}$Po, $^{208,209,210,211}_{85}$At, $^{210,211,212,213,214}_{86}$Rn, $^{208,211,212,213,214}_{87}$Fr, $^{210,211,212,214,215}_{88}$Ra and $^{215}_{89}$Ac following the projectile fragmentation of a 1 A.GeV ^{238}U beam by a ^{9}Be target at GSI Helmholtzzentrum für Schwerionenforschung. The fragments were separated in the fragment separator (FRS) and identified by means of energy loss and time-of-flight techniques. They were brought to rest at the centre of the RISING gamma-ray detector array and intensities of gamma-rays emitted in the decay of isomeric states with half-lives between 100 ns and 40 μs and spin values up to 55/2 $\hbar$ were used to obtain the corresponding isomeric ratios. The data are compared to theoretical isomeric ratios calculated in the framework of the abrasion-ablation model. Large experimental enhancements are obtained for high-spin isomers in comparison to expected values.

The need for an understanding of relativistic heavy-ion collisions spans a number of scientific fields, from the safety of human space exploration [1] and cosmic-ray astrophysics [2], to the structure of the early Universe [3] and the generation of radioactive ion beams [4]. Nevertheless, the complexity of the nuclear-reaction processes and the large number of possible product isotopes have resulted in only limited tests of reaction models, which have focused mainly on hydrodynamic properties [5], isotope yields [6], and momentum distributions [7].

In addition, the angular-momentum degree of freedom has the potential to reveal important aspects of the reaction dynamics. However, this requires special circumstances for study to be possible. Following a given collision, the excited nuclear products typically de-excite in less than 10^{-8} s. Such a short time is insufficient to apply separation techniques that would enable the initial excitation energies and angular momenta to be determined, since the de-excitation radiations all occur in close proximity to the reaction target.

A breakthrough came with the ability to separate the products of projectile-fragmentation reactions according to their mass and charge [8], combined with the detection of γ rays from nuclear isomeric states [9, 10]. Excellent sensitivity was achieved for isomer half-lives in the 0.1-100 μs range, after the recoiling ions had been transported to a remote measurement station in less than 1 μs. In the present context, a key feature of nuclear isomers is that in many cases they carry high angular momentum, which is itself closely associated with their extended half-

lives [11].

The measurement of isomer production probabilities following fragmentation reactions initially supported the validity of the model calculations [12, 13], with angular momenta up to 20 $\hbar$ being studied. However, when higher angular momenta were identified, a large production excess became apparent [14]. At that time, the evidence rested heavily on a single data point, from a 43/2 $\hbar$ isomer in ^{215}Ra. We now report extensive further measurements that conclusively establish remarkably strong populations of high-spin isomers, with angular momenta up to 55/2 $\hbar$. Increasing deviation compared to model calculations is found as angular momentum increases.

The nuclei of interest were studied at the Gesellschaft für Schwerionenforschung (GSI), Darmstadt, Germany and were produced in the projectile fragmentation of a pulsed ^{238}U beam accelerated to 1 A.GeV in the GSI SIS18 accelerator. The beam impinged on a ^{9}Be target and fully stripped fragments were separated in the GSI FRagment Separator (FRS) [8] in achromatic mode, using the $(B\rho)_1 - \Delta E - (B\rho)_2$ technique, and identified by means of time-of-flight and energy-loss techniques. The mass-to-charge ratio (A/q) was calculated from the magnetic rigidity of the particles, and the time-of-flight (ToF) measured between two scintillation detectors at the intermediate and final focal planes of the FRS. The atomic number of the fragment (Z) was calculated from the energy loss in two multi-sampling ionisation chambers, corrected for particle velocity and trajectory. These detectors were calibrated using the primary ^{238}U beam. The data presented in this letter were collected using four different FRS settings: centred on ^{212}Rn, ^{214}Th, ^{213}Fr and ^{214}Ra. The ^{9}Be target thicknesses and typical primary beam intensities were 2.5 g/cm^2 and 2 x 10^6 particles per second for the first two settings and 3 g/cm^2 and 1 x 10^8 for the other two.

At the end of the separator, the fragments were slowed by an Al degrader and implanted in a stopper. γ-rays emitted by the implanted nuclei were measured in the RISING γ-ray array, comprising 15 Cluster detectors, which has an efficiency of $\sim$ 15% for the 662-keV gamma rays emitted in the decay of ^{137}Cs [15]. The array was calibrated for energy using a composite gamma-ray source containing ^{241}Am,^{133}Ba,^{137}Cs and ^{60}Co. Data were collected using two different stoppers and the efficiency information for each has been obtained using a combination of GEANT4 [16] simulations and data obtained from the source placed on either side of the stopper. A detailed description of the performance of RISING in its stopped-beam configuration is given in [15, 17]. The acquisition system was triggered by the arrival of a fragment and remained 'open' for a time window of 100 μs. Fragments which did not implant triggered a scintillation detector behind the stopper and this provided a veto. In addition to the veto detector, other conditions imposed in the off-line analysis included the exclusion of events where the fragment changed its charge state during transmission through the separator and events where the fragment interacted with the degrader.

Following isotopic identification of each fragment, 2-d spectra of the energies of γ-rays measured in the RISING array and their emission time (relative to fragment deposition) were constructed. These were then analysed to obtain isomeric ratios (R_{exp}), determined from the total intensity of transitions depopulating an isomeric state and defined as [12]:

$$R_{exp} = \frac{Y}{N_{imp}FG}, \quad (1)$$

where N_{imp} is the number of ions implanted in the stopper, F and G are correction factors and Y is the observed decay yield calculated from measured gamma-ray intensities and corrected for electron conversion. The factor F corrects for the decay of the isomeric state as it travels through the FRS and depends on the ToF through the FRS and the corresponding Lorentz factors. This factor also takes account of any hindrance to the decay due to the ions being in a fully stripped state as they travel through the separator. The factor G corrects for the time window used in the off-line analysis to produce the delayed-gamma-ray spectra and accounts for the fact that only a fraction of the total decay is observed. The largest contribution to the error on R_{exp} is in the decay yield (Y) and is due to the low statistics in the gamma-ray spectra. The uncertainty in the implantation depth of the ion and hence in the gamma-ray absorption in the stopper is also included in this term. In some nuclei, more than one isomer was populated in the same nucleus and a lower-lying isomer could be fed by the delayed decay of the higher-lying isomer. In these cases the isomeric ratio of the lower-lying state has been corrected for the decay from the higher-lying isomer and the uncertainty on the upper value is included in the error on the lower value. Further details of this method and the relevant formulae are given in [12].

Table I lists the isomeric ratios measured in the current work calculated, in most cases, using more than one depopulating transition. In all cases, bar those of $^{210-212}$Ra, the half-life that has been used in the determination of the isomeric ratio is from the literature. From the current data it was possible to confirm these values but better accuracy could not be obtained. The values measured in the current work for ^{210,211}Ra, are in general agreement with previous values [20, 21] but have a smaller error and therefore have been used in the analysis. In the case of ^{212}Ra, half-lives of 480(40) ns and 7.1(2) μs for the $(11)^-$ and $(8)^+$ isomeric states respectively, have been measured in this experiment and used for the calculation of the isomeric ratios. The value obtained for the $(11)^-$ state is about half the value of 850(13) ns quoted in [18] while the value for the $(8)^+$ state compares with previous values of 9.1(6) μs in [21]

and 10.9(4) μs in [18] .

Although table I shows that there are 12 cases where the excitation energy of the isomeric state is unknown, there are only 3 (12^+ in ^{198,200}Po and $(55/2^+)$ in ^{213}Rn) where the unobserved transition depopulates the isomer directly and therefore affects the isomeric ratio. The effect of the multipolarity of the unobserved transition on the isomeric ratio was discussed in detail in [13] for the case of the 12^+ level in ^{198,200}Po. Table 2 of [13] shows that for a missing transition of energy $E_\gamma = 50$ keV, the multipolarity of the transition has no effect on the isomeric ratio (to 3 significant figures). The $(55/2^+)$ level in ^{213}Rn has the highest spin value for which an isomeric ratio has been measured in the current work. Fig. 1 shows the gamma-ray energy spectrum obtained in coincidence with implanted ^{213}Rn ions within a time gate of Δt = 50-1450 ns. The isomeric ratio for the $(55/2)^+$ level at y+5929 keV has been obtained from the intensity of the 1010 keV transition which is clearly observed in the figure. Assuming no in-flight decay, the isomeric ratio is 0.8(2) which is the same as would be obtained for an E2/M1 transition of 100 keV. If the transition were to be an E1, then the ratio increases to 1.3(4) which is the maximum value that it can take. The lower value of 0.8(2) is used in the table and subsequent discussion. Most of the other strong transitions in the spectrum in Fig. 1 have been used to obtain isomeric ratios for other lower-lying isomeric states as listed in Table I.

Table I also lists the isomeric ratios measured for these states in previous works. In the case of the Po nuclei, the values measured in the current work agree with those measured by Gladnishki et al. [13] to within 2 standard deviations. However in the case of the Fr and Ra nuclei measured in [14], there is a factor of at least 2 between the values presented here and previous ones, with those in the current work being larger. The results presented in both [13] and [14] used the same reaction at the same experimental facility although Gladnishki [13] et al. used a beam energy of 750 A.MeV and Podolyák et al. [14] 900 A.MeV. At the higher beam energy (1 A.GeV) used in the current experiment, there were fewer problems with contamination and with charge state identification, and therefore the isotopic identification should be cleaner and the data more reliable. It should also be noted that the experimentally observed value is always a lower limit as there is a possibility that some of the higher-spin population bypasses the measured isomer.

Fig. 2 shows a comparison of the experimental isomeric ratios obtained in the current work with theoretical values calculated using the macroscopic abrasion-ablation (ABRABLA) model [46, 47](shaded data points) and the relativistic transport-statistical sequential binary decay (ART+SBD) [19] model (open circles). Although the distribution of data points makes a firm cut-off point difficult to establish, Fig. 2 indicates that there is reasonable agreement between the experimental values and

TABLE I. Summary of the measured isomeric ratios ordered by increasing Z and A. The third last column contains the results of previous measurements and the last two columns calculated values. Data obtained for Po from [22–25], for At from [26–30], for Rn from [31–35], for Fr from [20, 36–41], for Ra from [18, 20, 21, 42–44] and for Ac from [45].

^{A}Z	I^π	E_{lev} (keV)	$t_{1/2}$ (μs)	R_{exp} (%) this work	[13, 14]	ρ_{the} (%) this work	[19]
^{198}Po	12^+	x+2692	0.75(5)	4(2)[a]	9(1)	30	
	11^-	2566	0.20(2)	20(5)[a]		36	
^{200}Po	12^+	x+2804	0.268(3)	7(3)[a]	7(1)	27	
	11^-	2596	0.104(9)	48(23)[a]	39(4)	33	
^{206}Po	9^-	2262	1.05(6)	15(2)[a]		37	
	8^+	1586	0.232(4)	12(2)		44	
^{208}Po	8^+	1528	0.35(2)	27(2)		42	
^{208}At	16^-	2276	1.5(2)	8.6(9)		5.8	
^{209}At	$(29/2)^+$	2429	0.89(4)	17(1)		7.2	
^{210}At	19^+	4028	5.66(7)	8.9(9)		1.7	
	15^-	2550	0.482(6)	5.2(7)		6.5	
^{211}At	$39/2^-$	4815	4.2(4)	6.6(4)		1.2	
^{210}Rn	$(17)^-$	x+3812	1.06(5)	10(1)		3.9	
	(8^+)	x+1665	0.64(4)	19(5)		43	
^{211}Rn	$35/2^+$	x+3926	0.040(1)	14(3)		2.7	
	$17/2^-$	x+1578	0.60(3)	38(3)		33	
^{212}Rn	22^+	6174	0.109(5)	3.4(5)		0.5	
	8^+	1694	0.91(3)	34(2)		39	
^{213}Rn	$(55/2^+)$	y+5929	0.16(1)	0.8(2)[a] [b]		0.031(5)	
	$43/2^-$	x+3495	0.028(1)	9(5)[a]		0.5	
	$31/2^-$	x+2187	1.36(7)	17(2)[a]		4	
	$25/2^+$	x+1664	1.0(2)	6(3)		11	
^{214}Rn	(22^+)	4595	0.25(3)	4.8(9)		0.5	
^{208}Fr	10^-	826	0.43(1)	16(1)		32	
^{211}Fr	$45/2^-$	4657	0.12(1)	2.8(3)		0.4	
	$29/2^+$	2423	0.15(1)	16(1)	6(2)	7.1	10.0
^{212}Fr	15^-	2492	0.58(2)	19(1)	8(2)	6.8	9.2
	11^+	1551	27.1([c])	21(2)		22	
^{213}Fr	$29/2^+$	2538	0.238(6)	23(2)	12(8)	6.5	10.8
	$21/2^-$	1590	0.51(1)	22(2)		21	
^{214}Fr	11^+	638	0.103(4)	69(10)[a]		20	
^{210}Ra	8^+	2050	2.1(1) [d]	31(2)		43	
^{211}Ra	$(13/2^+)$	1198	9.4(4) [d]	35(2)		52	
^{212}Ra	$(11)^-$	2613	0.48(4) [d]	25(2)		20	
	$(8)^+$	1958	7.1(2)[d]	18(2)		41	
^{214}Ra	17^-	4147	0.225(4)	13(1)[a]	7(2)	2.3	3.2
	14^+	3478	0.279(4)	13(1)		7	
	8^+	1865	68(1)	64(2)		38	
^{215}Ra	$(43/2^-)$	x+3757	0.55(1)	7.9(8)	3.1(6)	0.21	0.8
^{215}Ac	$(29/2^+)$	x+2438	0.34(1)	20(4)[a]	5(1)	3.7	
	$21/2^-$	1796	0.19(3)	20(5)		15	

[a] The intensity of only one transition has been used in equation 1 to calculate the isomeric ratio.

[b] Statistical error, assuming no in-flight decay. The corresponding values of R_{exp} for an E2/M1 or E1 decay of 100 keV are 0.8(2) and 1.3(4) respectively. The latter value is the maximum possible compatible with the lack of observation.

[c] No error is quoted in the original reference [38].

[d] The half-life measured in this work has been used in the analysis.

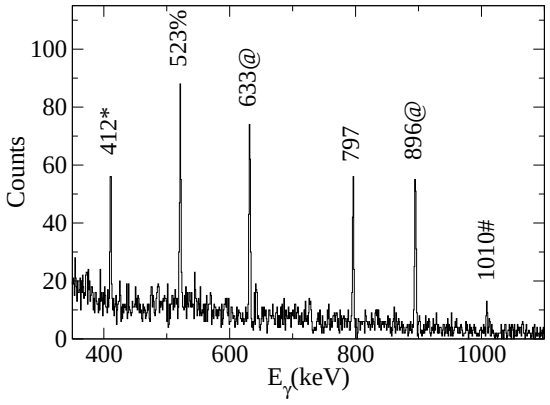

FIG. 1. Gamma-ray energy spectrum obtained in coincidence with ^{213}Rn ions using a time gate of width 1.4 μs starting $\sim$ 50 ns after the prompt flash. The transitions used to obtain the isomeric ratios for the $(55/2)^+$, $43/2^-$, $31/2^-$ and $25/2^+$ levels are denoted #,*,% and @ respectively.

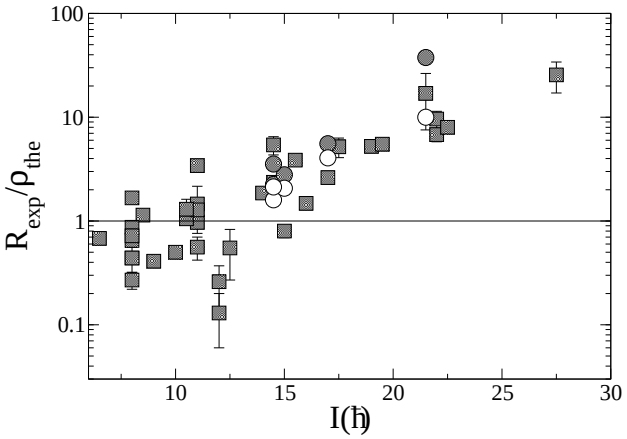

FIG. 2. The ratio of the experimental isomeric ratios observed in this work to values calculated using the ABRABLA model (shaded symbols) and the ART+SBD [19] model (open circles). The open/shaded circles show a direct comparison of the different theoretical values for the same experimental value.

those calculated by the ABRABLA code for spin values $\leq$13 $\hbar$. For spin values greater than this, both codes underestimate the level population by a factor which seems to increase in an approximately linear manner with the logarithmic scale in Fig. 2, i.e. suggesting an exponential dependence. The figure also shows that there is a range of isomeric ratios for each value of spin and that while the values measured by [14] (discussed above) differ somewhat from the values measured in the current work, they are not outside the overall band. It should be noted that an analogous graph plotted against excitation energy shows the same trend of increasing underestimation by the models as the energy increases.

In the ABRABLA model [46, 47], the fragmentation process is considered in two steps, an ABRasion stage where there is a clean cut of both the target and the projectile and the angular momentum generated in the target fragment is dependent solely on the angular momentum of the removed nucleons. In the ABLAtion stage, the excited prefragment either fissions or emits nucleons. In the case of the nuclei discussed here, it is the nucleon emission process that is relevant and once below the particle emission threshold, the nuclei continue to cool via the statistical emission of gamma-rays. This part of the decay is modelled using Monte Carlo codes and, on average, does not change the angular momentum of the fragment. The underestimation of the data by the ABRABLA model was pointed out in [14] and attributed to the lack of inclusion of any collective effect in the angular momentum generation. Such an effect could originate from a type of friction or viscosity as the target and projectile pass through each other. An attempt was made to estimate the magnitude of this effect in [14] and it was shown to make a sizeable difference (a factor of 4 at spin 43/2 $\hbar$). The new measurements for I>20$\hbar$, presented here, now demand a more sophisticated theoretical treatment. We speculate that the exponential nature of the experimental enhancement could perhaps also be due to the level density term in the calculations, which does have this form and has not been validated at such high excitation energies.

The subsequent development of the ART+SBD model [19] also did not include any collective features. Although it uses a relativistic transport model to describe the size and excitation energy of the prefragment, the initial angular momentum is again generated only from single-particle excitations. This distribution is then broadened in the sequential binary decay process. While Table I shows that the ratios predicted using this model are systematically higher than those using ABRABLA, they also underestimate the data (by a factor ranging from $\sim$2 at spin 14 $\hbar$ to $\sim$10 at spin 21 $\hbar$). No ART+SBD predictions are currently available for the isomeric ratio for the 55/2 $\hbar$ state measured in this work.

In summary, isomeric ratios for states with spin values between 13/2 and 55/2 $\hbar$, in neutron-deficient N$\sim$126 nuclei produced in projectile fragmentation reactions, have been measured at the GSI facility. Although the data show the expected decrease of the isomeric ratio as a function of spin, this decrease is much slower than predicted by model calculations, an effect which could be due to the lack of a collective component in current models. Given the recent increase in the number and diversity of beams which are being produced by fragmentation, it is

important that this discrepancy is investigated and understood in the near future.

ACKNOWLEDGMENTS

This work is supported by the STFC(UK), AWE plc, the Bulgarian National Science Fund (DMU02/1-06.01.2010), the Hungarian Scientific Research Fund (OTKA K100835), the Polish Ministry of Science and Higher Education (1-P03B-030-30 and 620/E-77/SPB/GSI/P-03/DWM105/2004-2007), the Spanish Ministerio de Educación y Ciencia (FPA2005-00696 and FPA2006-12431), the Swedish Science Council, the DFG (EXC 153), the German Federal Ministry of Education and Research (06KY205I) and EURONS (EU contract number 506065).

* Present address: Comisión Chilena de Energía Nuclear, Casilla 188-D, Santiago, Chile

[1] Marco Durante and Francis A.Cucinotta, Nature Reviews Cancer 8 (2008) 465 and Reviews of Modern Physics 83 (2011) 1245
[2] F. Gahbauer et al., Astron. J. 607 (2004) 333
[3] M.Di Toro *et al.,* J. Phys. G37 (2010) 083101
[4] D.F. Geesaman, C.K. Gelbke, R.V.F. Janssens, and B.M. Sherrill, Ann. Rev. Nucl. Part. Sci. 56 (2006) 53
[5] W.G. Lynch, Ann. Rev. Nucl. Part. Sci. 37 (1987) 493
[6] H. Alvarez-Pol et al., Phys. Rev. C 82 (2010) 041602(R)
[7] T. Enquist *et al.,* Nucl. Phys. A658 (1999) 47
[8] H. Geissel, Nucl. Instr. Meth. Phys. Res. B70 (1992) 286
[9] R. Grzywacz et al., Phys. Lett. B 355 (1995) 439
[10] M. Pfützner et al., Phys. Lett. B 444 (1998) 32
[11] P.M. Walker and G.D. Dracoulis, Nature 399 (1999) 35
[12] M. Pfützner et al., Phys. Rev. C65 (2002) 064604
[13] K. Gladnishki *et al.*, Phys. Rev. C69 (2004) 024617
[14] Zs. Podolyák *et al.,* Phys. Lett. B632 (2006) 203
[15] S. Pietri *et al.,* Nucl. Instr. Meth. Phys. Res. B261 (2007) 1079; S. Pietri *et al.,* Acta Phys. Polonica B38 (2007) 1255
[16] S. Agostinelli *et al.,* Nucl. Instr. Meth. Phys. Res. A506 (2003) 250
[17] P. Regan *et al.,* AIP Conf.Proc. 899 (2007) 19
[18] T. Kohno *et al.*, Phys. Rev. C33 (1986) 392
[19] S. Pal and R. Palit, Phys. Lett. B665 (2008) 164
[20] Zs. Podolyák *et al.,* AIP Conf. Proc. 831 (2006) 114
[21] K. Hauschild *et al.,* Nucl. Instr. Meth. Phys. Res. A560 (2006) 388
[22] A. Maj *et al.,* Nucl. Phys. A509 (1990) 413
[23] T. Weckstrom *et al.,* Z. Phys. A321 (1985) 231
[24] A.M. Baxter *et al.,* Nucl. Phys. A515 (1990) 493
[25] O. Häusser *et al.,* Nucl. Phys. A273 (1976) 253
[26] B. Fant *et al.,* Nucl. Phys. A429 (1984) 296
[27] M.J. Martin Nucl. Data Sheets 63 (1991) 723
[28] E. Browne Nucl. Data Sheets 99 (2003) 649
[29] K.H. Maier *et al.,* Phys. Lett. B35 (1971) 401
[30] S. Bayer *et al.,* Nucl. Phys. A694 (2001) 3
[31] A.R. Poletti *et al.,* Nucl. Phys. A359 (1981) 180
[32] E. Browne Nucl. Data Sheets 104 (2005) 427
[33] A.E. Stuchbery *et al.,* Nucl. Phys. A482 (1988) 692
[34] G.D. Dracoulis *et al.,* Nucl. Phys. A467 (1987) 305
[35] T. Lönnroth *et al.,* Phys. Rev. C27 (1983) 180
[36] G.D. Dracoulis *et al.,* Eur. Phys.Jour. A40 (2009) 127
[37] A.P. Byrne *et al.,* Nucl. Phys. A448 (1986) 137
[38] J.R. Beene *et al.,* Hyperfine Interactions 3 (1977) 397
[39] O. Häusser *et al.,* Phys. Lett. B63 (1976) 279
[40] M.E. Debray *et al.*, Phys. Rev. C48 (1993) 2246
[41] A.P. Byrne *et al.,* Nucl. Phys. A567 (1994) 445
[42] A.E. Stuchbery *et al.,* Nucl. Phys. A548 (1992) 159
[43] S.C. Wu Nucl. Data Sheets 110 (2009) 681
[44] A.E. Stuchbery *et al.,* Nucl. Phys. A641 (1998) 401
[45] D.J.Decman *et al.,* Z. Phys. A310 (1983) 55
[46] J.-J.Gaimard and K.-H.Schmidt Nucl. Phys. A531 (1991) 709
[47] M. de Jong, A.Ignatyuk and K.-H.Schmidt Nucl. Phys. A613 (1997) 435